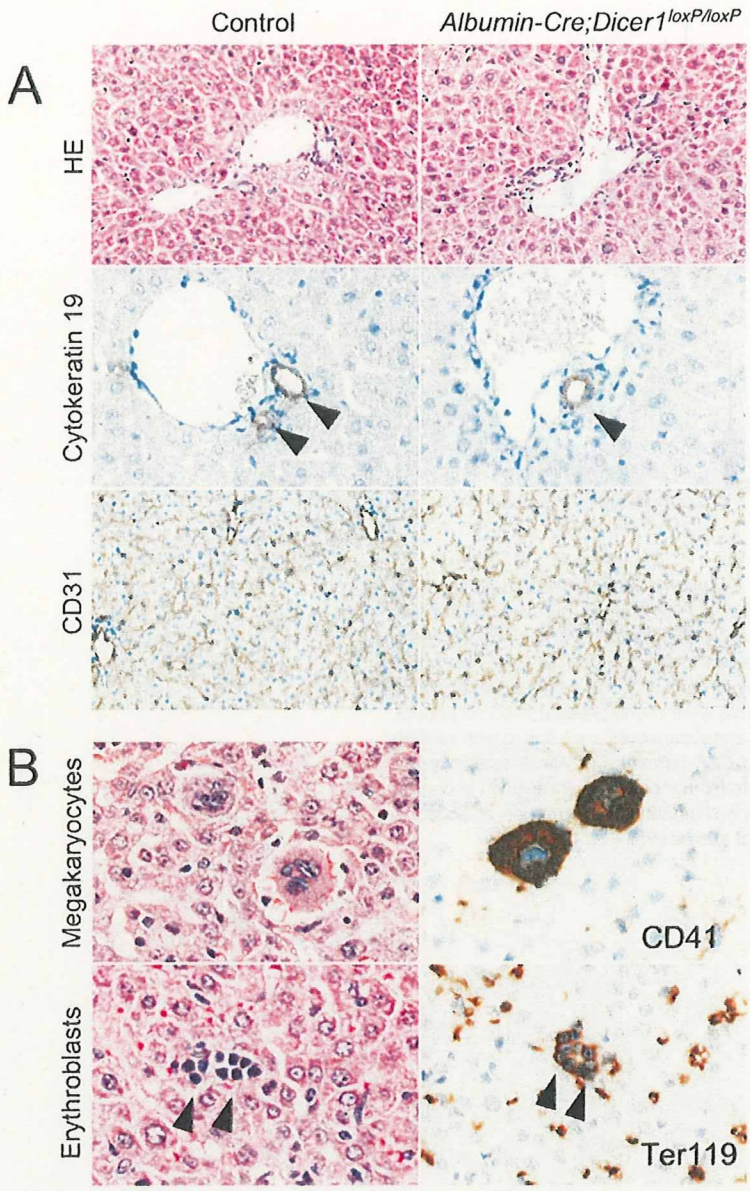

Supplementary Figure 2. Nonparenchymal cell components of *Albumin-Cre;Dicer1*$^{loxP/loxP}$ mouse livers. (*A*) Histologically, *Albumin-Cre;Dicer1*$^{loxP/loxP}$ mouse livers did not show significant alterations in portal tract morphology. Staining for cytokeratin 19 to stain bile ducts and CD31 to highlight endothelial cells did not reveal significant abnormalities. (*B*) Hematopoietic cell colonization, which is not observed in controls, was found in most *Albumin-Cre;Dicer1*$^{loxP/loxP}$ mouse livers. The presence of megakaryocytes was confirmed by staining for CD41. Islands of erythroblasts were also noted (*arrowheads*). Ter119 was positive in both erythroblasts and mature erythrocytes, but immature erythroblasts were distinguished by the presence of nuclei (*arrowheads*).

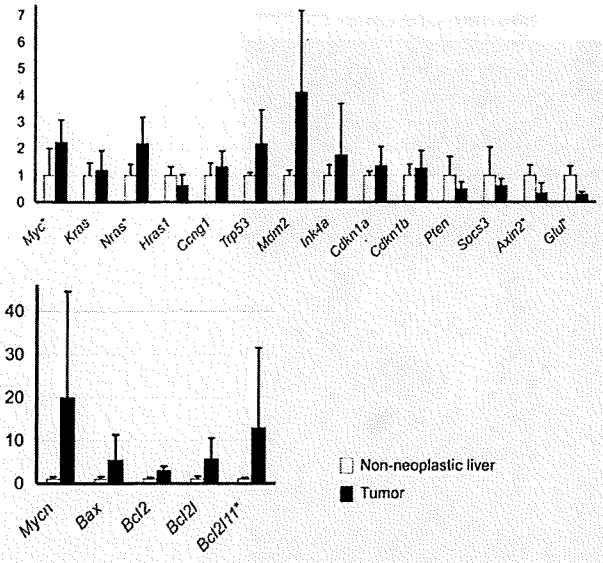

Supplementary Figure 3. Expression of tumor-related genes in *Dicer1*-deficient HCCs. Quantitative PCR analysis of nonneoplastic liver samples and HCCs from *Albumin-Cre;Dicer1*$^{loxP/loxP}$ (n = 6–8 for each group). Values are expressed as mean ± SD. $^{*}P < .05$. Two oncogenes, *Myc* and *Nras*, were significantly but only modestly up-regulated in HCCs. While *Mycn* and *Bcl2* were overexpressed in some tumors, the differences did not reach statistical significance due to high variability. Expression of *Axin2* and *Glul*, hallmarks of Wnt/β-catenin signal activation, was down-regulated in tumors. This observation is consistent with the absence of *Ctnnb1* mutations. Expression of *Socs3*, a major target of Stat3, was not altered in HCCs.

Journal of Pathology
J Pathol 2009; **219**: 365–372
Published online 27 July 2009 in Wiley InterScience
(www.interscience.wiley.com) **DOI:** 10.1002/path.2606

Original Paper

Dicer is required for proper liver zonation

Shigeki Sekine,[1]* Reiko Ogawa,[1] Michael T Mcmanus,[2] Yae Kanai[1] and Matthias Hebrok[2]
[1]*Pathology Division, National Cancer Center Research Institute, Tokyo, Japan*
[2]*Diabetes Center, Department of Medicine, University of California San Francisco, San Francisco, California, USA*

**Correspondence to:*
Shigeki Sekine, Pathology Division, National Cancer Center Research Institute, 5-1-1, Tsukiji, Chuo-ku, Tokyo, Japan.
E-mail: ssekine@ncc.go.jp

No conflicts of interest were declared.

Received: 21 June 2009
Revised: 17 July 2009
Accepted: 17 July 2009

Abstract

A number of genes and their protein products are expressed within the liver lobules in a region-specific manner and confer heterogeneous metabolic properties to hepatocytes; this phenomenon is known as 'metabolic zonation'. To elucidate the roles of Dicer, an endoribonuclease III type enzyme required for microRNA biogenesis, in the establishment of liver zonation, we examined the distribution of proteins exhibiting pericentral or periportal localization in hepatocyte-specific *Dicer1* knockout mouse livers. Immunohistochemistry showed that the localization of pericentral proteins was mostly preserved in *Dicer1*-deficient livers. However, glutamine synthetase, whose expression is normally confined to a few layers of hepatocytes surrounding the central veins, was expressed in broader pericentral areas. Even more striking was the observation that all the periportal proteins that were examined, including phosphoenolpyruvate carboxykinase, E-cadherin, arginase 1, and carbamoyl phosphate synthetase-I, lost their localized expression patterns and were diffusely expressed throughout the entire lobule. Thus, with regard to periportal protein expression, the consequences of Dicer loss were similar to those caused by the disruption of β-catenin. An analysis of livers deficient in β-catenin did not identify the down-regulation of *Dicer1* or any microRNAs, indicating that they are not directly activated by β-catenin. Thus, the present study illustrates that Dicer plays a pivotal role in the establishment of liver zonation. Dicer is essential for the suppression of periportal proteins by Wnt/β-catenin/TCF signalling, albeit it likely acts in an indirect manner.

Keywords: Dicer; β-catenin; liver; zonation

Introduction

Although hepatocytes are uniform at a histological level, they differ in a number of metabolic functions [1,2]. For example, pericentral hepatocytes are active in glutamine and bile acid synthesis and the metabolism of xenobiotics, whereas periportal hepatocytes are more active in cholesterol, urea, and glucose synthesis [1,2]. The metabolic heterogeneity of hepatocytes enables multiple and occasionally antagonistic metabolic functions to be performed efficiently in the liver. A number of genes and their protein products involved in these metabolic processes are expressed in a region-specific manner along the porto-central axis within the liver lobule and their respective functions confer the heterogeneous metabolic properties of hepatocytes [1–3].

Recent studies have revealed that the Wnt signalling pathway plays a key role in the establishment of liver zonation [4,5]. The Wnt signalling pathway is activated by the binding of secreted Wnt ligands to Frz and Lrp receptors on cell membranes. This leads to the stabilization of β-catenin through the inhibition of proteosomal degradation, and the translocation of the protein to the nucleus, where it activates TCF-dependent transcription [6]. β-Catenin/TCF-dependent transcription is normally active in the pericentral hepatocytes, where it induces pericentral gene expression while suppressing periportal gene expression [4,7]. The hepatocyte-specific ablation of Apc, leading to the constitutive activation of β-catenin/TCF-dependent transcription, resulted in the diffuse expression of pericentral genes and the down-regulation of periportal genes throughout the entire liver lobule [4,8]. Conversely, the suppression of Wnt signalling by the overexpression of Dkk1 or the conditional ablation of β-catenin caused a loss of pericentral gene expression and the diffuse expression of periportal genes [4,9]. Braeuning *et al* further showed that activation of the Ras/MAPK pathway by the oncogenic form of H-ras or serum components suppressed pericentral genes and induced periportal genes through the inhibition of β-catenin/TCF-dependent transcription [10,11]. Thus, the expression of pericentral and periportal genes is coordinately and inversely regulated by Wnt/β-catenin/TCF signalling.

Dicer is an essential component of microRNA biogenesis that cleaves pre-microRNAs into mature microRNAs. Since Dicer is encoded by a single locus in the mouse genome, the disruption of the single *Dicer1* gene results in the loss of virtually all microRNAs [12–14]. Here, we demonstrate that Dicer plays an essential role in the establishment of proper liver zonation. Remarkably, the loss of Dicer impairs the localization of periportal proteins, leaving the expression of pericentral proteins mostly intact. Thus, our results reveal the novel finding that microRNAs appear to be specifically required for the suppression of periportal protein expression.

Materials and methods

Mice

Alb-Cre [15,16], *Dicer1*$^{flox/flox}$ [12], *Ctnnb1*$^{flox/flox}$ [17], *Alb-Cre;Ctnnb1*$^{flox/flox}$ [7,9], and *Alb-Cre;Dicer*$^{flox/flox}$ [18] mice have been previously described. The mice used in the present study were maintained in barrier facilities and all studies were conducted in compliance with the University of California IACUC (Institutional Animal Care and Use Committee) guidelines and according to protocols approved by the Committee for Ethics in Animal Experimentation at the National Cancer Center, Japan.

Immunohistochemistry

Liver tissue samples were fixed with 10% buffered formalin, embedded in paraffin, and cut into 5-μm-thick sections. Immunohistochemistry was performed by an indirect immunoperoxidase method using peroxidise-labelled anti-mouse, -rabbit or -goat polymers (Histofine Simple Stain, Nichirei, Tokyo, Japan). 3,3′-Diaminobenzidine tetrahydrochloride was used as a chromogen. The primary antibodies that were used are listed in Table 1. For double immunofluorescence staining, anti-mouse IgG antibody conjugated with Alexa Fluor 488 and anti-rabbit IgG antibody conjugated with Alexa Fluor 594 were used as secondary antibodies. The sections were analysed using a confocal microscope (LSM5 Pascal; Carl Zeiss Jena GmbH, Jena, Germany) equipped with a 15 mW Kr/Ar laser.

Quantitative PCR

RNA extraction and the reverse-transcription reaction were performed using standard protocols. Quantitative PCR reactions were performed using SYBR Green PCR master mix (Applied Biosystems, CA, USA). The expression of *Dicer1* was compared with the expression level of *Gusb*, as previously described [9]. The primer sequences were as follows: *Dicer1*: GAACGAAATGCAAGGAATGGA and GGGACTTCGATATCCTCTTCTTTCTC; *Gusb*: ACGGGATTGTGGTCATCGA and TCGTTGCCAAAACTCTGAGGTA.

Microarray analysis

RNA samples were prepared from liver tissues of 6-week-old female *Alb-Cre;Ctnnb1*$^{flox/flox}$ and *Ctnnb1*$^{flox/flox}$ mice. The samples were labelled with a miRNA Labeling Reagent & Hybridization Kit (Agilent Technologies, CA, USA) based on the manufacturer's instructions. The labelled RNA samples were hybridized with a mouse miRNA microarray (Agilent Technologies) containing 566 mouse miRNA probes based on Sanger miRBase v10.0. MicroRNAs that showed more than two-fold changes with $p < 0.05$ (Welch t-test) were considered significant.

Results

Localization of pericentral proteins is only marginally affected in Dicer mutant mice

To elucidate the roles of Dicer in liver zonation, liver samples from *Alb-Cre;Dicer*$^{flox/flox}$ mice and their control littermates (*Dicer*$^{flox/flox}$) were immunohistochemically examined. As previously reported, the efficient deletion of *Dicer1* in hepatocytes was achieved in 3-week-old *Alb-Cre;Dicer*$^{flox/flox}$ mice; however, *Dicer1*-deficient hepatocytes were prone to apoptosis and the complete disruption of *Dicer1* was followed by repopulation with *Dicer1*-expressing hepatocytes that had escaped Cre-mediated recombination [18]. We therefore examined the livers from 3-week-old *Alb-Cre;Dicer*$^{flox/flox}$ and *Dicer*$^{flox/flox}$ mice (hereafter referred to as Dicer-deficient and control livers).

Immunohistochemistry showed that the localization of pericentral proteins was mostly maintained

Table 1. Antibodies used for immunohistochemistry

Antigen	Clone	Dilution	Source
Glutamine synthetase	6	1:1000	Becton Dickinson, Franklin Lakes, USA
GLT-1	Polyclonal	1:500	Dr Masahiko Watanabe [24]
OAT	Polyclonal	1:500	Santa Cruz Biotechnologies, Santa Cruz, USA
CYP2E1	Polyclonal	1:500	Dr Magnus Ingelman-Sundberg [25]
E-cadherin	36	1:250	Becton Dickinson, Franklin Lakes, USA
PEPCK	Polyclonal	1:200	Santa Cruz Biotechnologies, Santa Cruz, USA
CPS1	Polyclonal	1:500	Santa Cruz Biotechnologies, Santa Cruz, USA
Arginase 1	19	1:2500	Becton Dickinson, Franklin Lakes, USA

OAT = ornithine aminotransferase; PEPCK = phosphoenolpyruvate carboxykinase; CPS1 = carbamoyl phosphate synthetase-I.

in the absence of Dicer. The distributions of GLT-1, ornithine aminotransferase (OAT), and CYP2E1 were unaltered in Dicer-deficient livers. GLT-1 and OAT were expressed in a few layers of hepatocytes surrounding the central veins (Figures 1A, 1B, 1D, and 1E). CYP2E1 was expressed in broader pericentral areas (Figures 1J and 1K). Expression of glutamine synthetase (GS) was observed in the pericentral areas of both mice; however, the GS-positive areas were significantly broader in the Dicer-deficient livers (Figures 1G and 1H).

The altered localization of GS was confirmed by double immunofluorescence staining for GS and CYP2E1. In control mouse livers, distinct distributions of these proteins were evident: GS expression was restricted to a few layers of hepatocytes surrounding the central veins, whereas CYP2E1 expression was extended to the distal pericentral

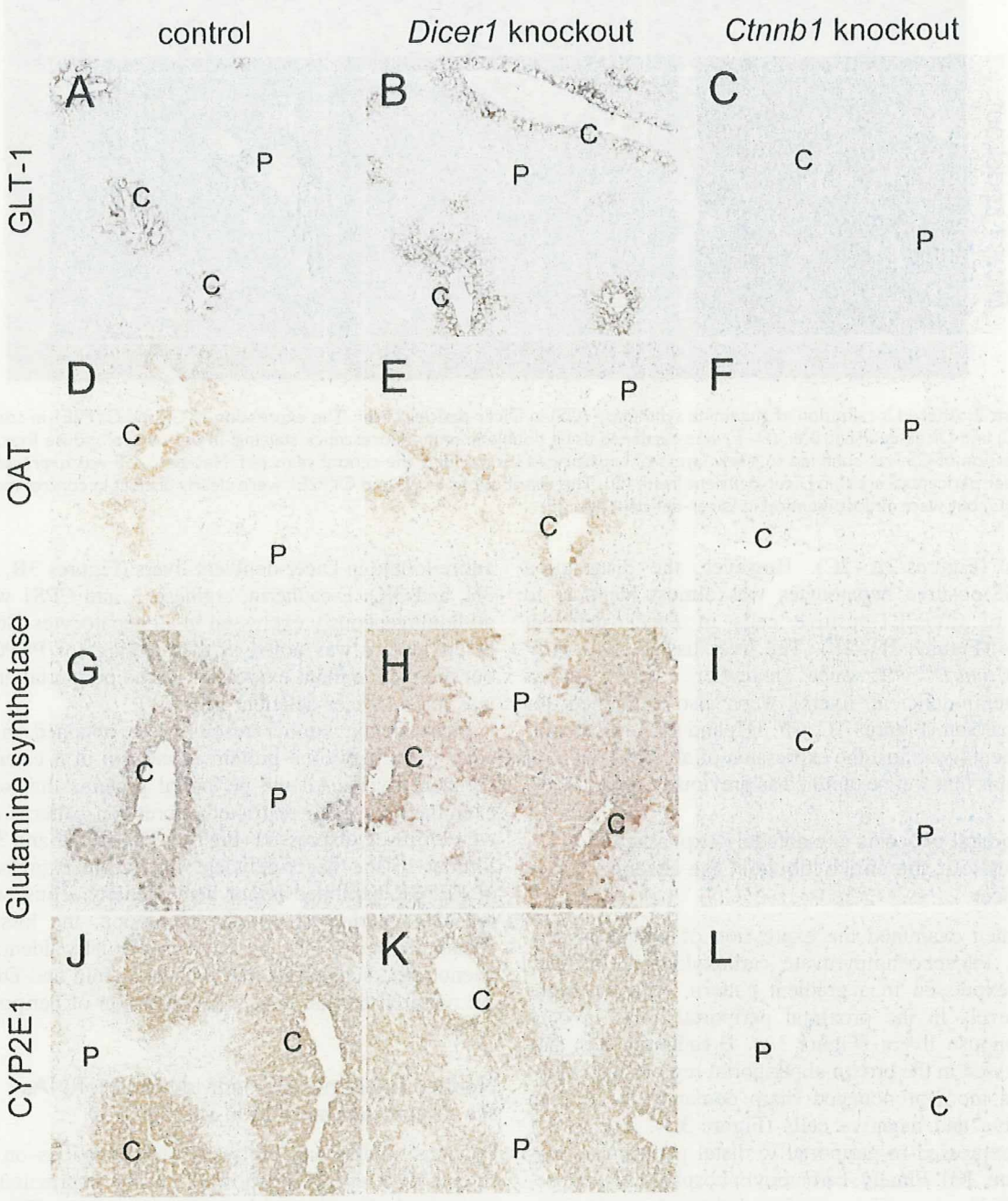

Figure 1. Expression of pericentral proteins in Dicer-deficient liver. Pericentral protein expression was examined using immunohistochemistry. The distributions of GLT-1, OAT, and CYP2E1 were unaltered in Dicer-deficient liver (B, E, K) compared with those in control mouse liver ($Dicer^{flox/flox}$) (A, D, J). Glutamine synthetase maintained its pericentral localization in Dicer-deficient liver (H), but its expression extended beyond its normal boundary and encompassed a broader area than that observed in control mouse liver (G). Pericentral protein expression was completely lost in β-catenin-deficient livers (C, F, I, L). C = pericentral vein; P = portal tract

J Pathol 2009; **219**: 365–372 DOI: 10.1002/path

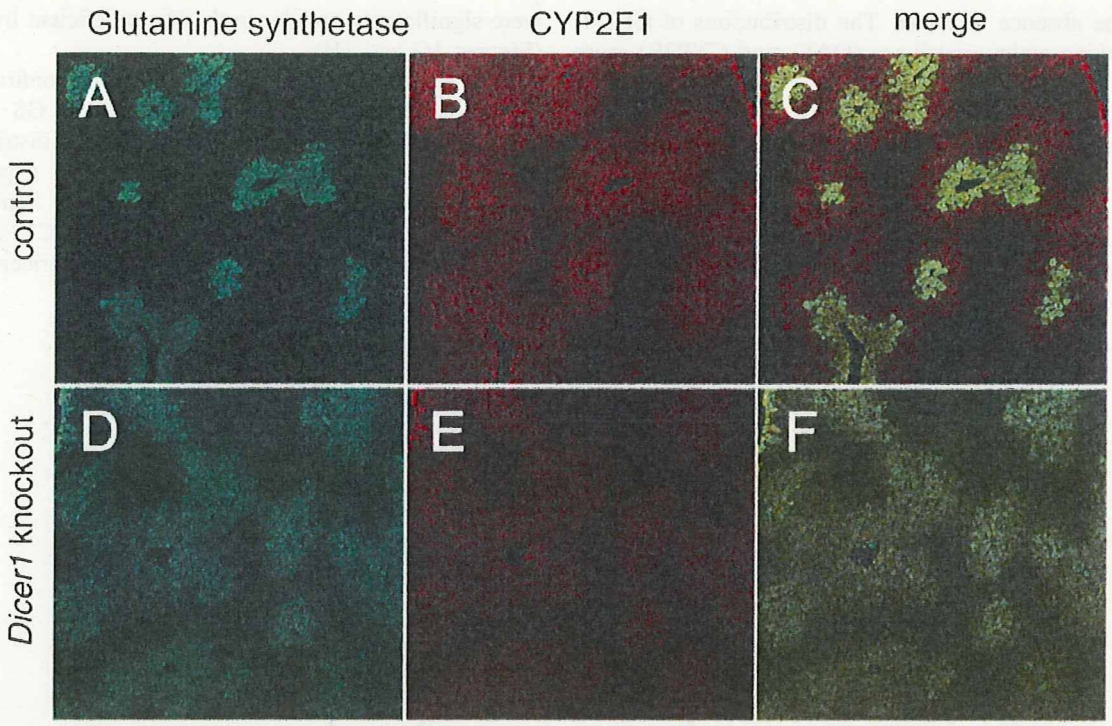

Figure 2. Altered localization of glutamine synthetase (GS) in Dicer-deficient liver. The expression of GS and CYP2E1 in control (A–C) and Dicer-deficient liver (D–F) was examined using double immunofluorescence staining. In the control mouse liver, the expression of GS was confined to a few layers of hepatocytes surrounding the central veins (A). However, GS was expressed in broader pericentral areas in Dicer-deficient livers (D). The distributions of GS and CYP2E1 were clearly distinct in control mouse liver (C) but were almost identical in Dicer-deficient liver (F)

areas (Figures 2A–2C). However, the distribution of GS-positive hepatocytes was almost identical to that of CYP2E1-positive cells in *Dicer1*-deficient livers (Figures 2D–2F). The liver tissues from *Alb-Cre;Ctnnb1*$^{flox/flox}$ mice (hereafter referred to as β-catenin-deficient livers) were also examined for comparison (Figures 1C, 1F, 1H, and 1K). β-Catenin-deficient livers lost the expression of all the pericentral proteins that were examined as previously reported [9].

Periportal proteins are diffusely expressed throughout the entire lobule in the absence of Dicer

We then examined the expression of periportal proteins. Phosphoenolpyruvate carboxykinase (PEPCK) was expressed in a gradient pattern, with the highest levels in the proximal periportal areas in control mouse livers (Figure 3A). E-cadherin was also expressed in the proximal periportal regions but exhibited a more pronounced sharp demarcation between positive and negative cells (Figure 3D). Arginase 1 was expressed in periportal to distal pericentral areas (Figure 3G). Finally, carbamoyl phosphate synthetase-I (CPS1) expression was found throughout the liver lobules, with the exception of a few layers of perivenous hepatocytes; this distribution was complementary to that of GS (Figure 3J). Remarkably, all of these periportal proteins lost their localized expression patterns and appeared in a diffuse pattern throughout the entire lobule in Dicer-deficient livers (Figures 3B, 3E, 3H, and 3K). E-cadherin, arginase 1, and CPS1 were all homogeneously expressed in all hepatocytes. Some heterogeneity was noted in the staining for PEPCK, but the predominant expression in the periportal areas was lost in Dicer-deficient livers.

Interestingly, similar results were obtained in an analysis of periportal protein expression in β-catenin-deficient livers. All the periportal proteins that were examined lost their restricted expression patterns and were diffusely expressed (Figures 3C, 3F, 3I, and 3L). Similar to the Dicer-deficient livers, the expression of PEPCK exhibited minor heterogeneity. Thus, with regard to periportal protein expression, the loss of β-catenin and Dicer resulted in virtually identical phenotypes, suggesting that both β-catenin and Dicer are required for the localized expression of periportal proteins.

Neither *Dicer1* nor any individual microRNAs are directly activated by β-catenin/TCF

Previous studies and the present observations on β-catenin-deficient livers showed that the expression of pericentral proteins is dependent on active Wnt/β-catenin signalling [4,9]. The conserved pericentral protein expression therefore indicates that Wnt signalling is still active in the pericentral hepatocytes of Dicer-deficient livers. On the other hand, periportal proteins are diffusely expressed throughout the liver lobules in

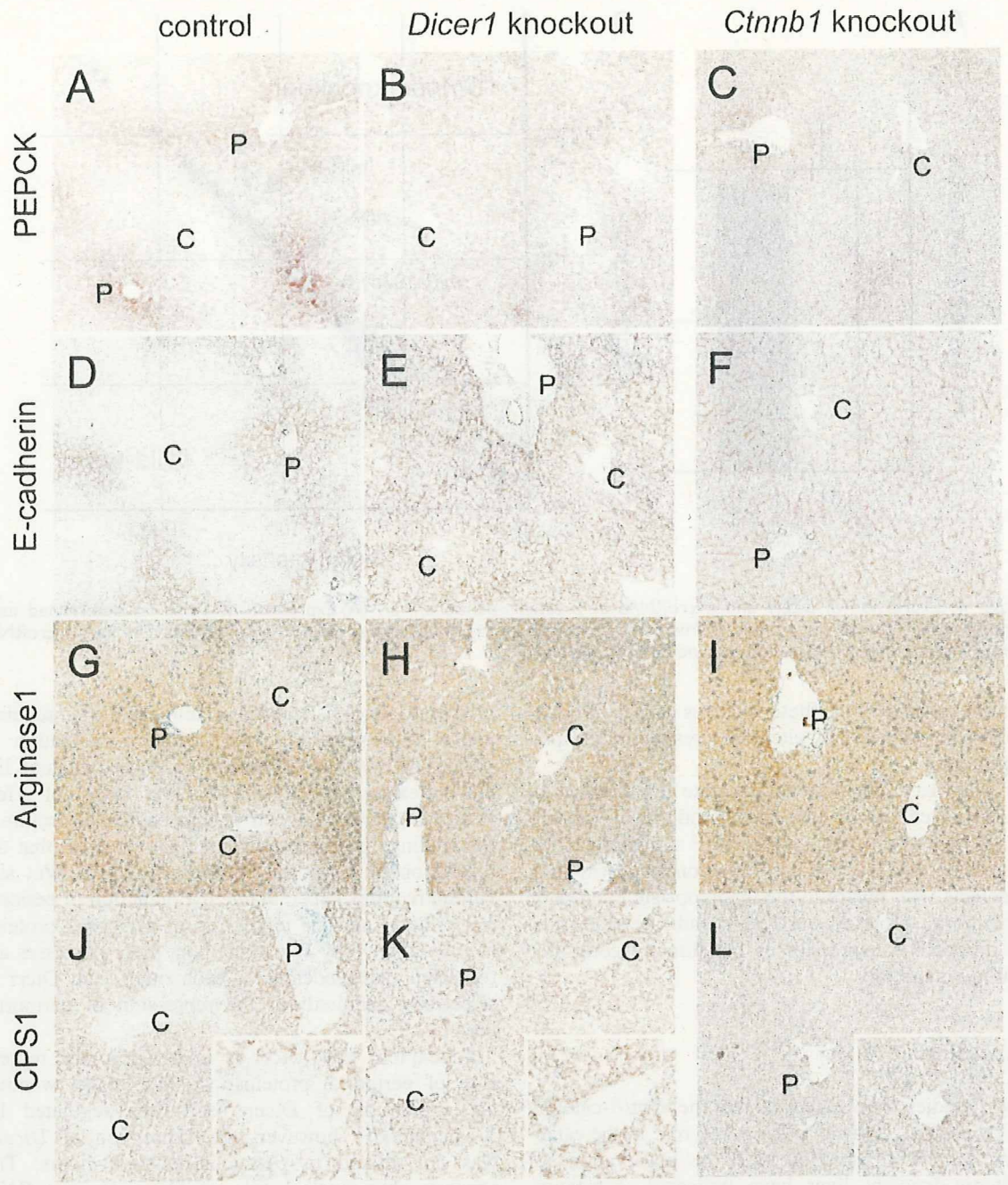

Figure 3. Expression of periportal proteins in Dicer-deficient liver. Periportal protein expression was examined using immunohistochemistry. The characteristic distributions of the periportal proteins in the control mouse liver (A, D, G, J) were completely lost in the Dicer-deficient (B, E, H, K) and β-catenin-deficient livers (C, F, I, L). High-magnification views of the pericentral areas are presented as insets for CPS1 (J–L). C = pericentral vein; P = portal tract

Dicer-deficient livers. This finding suggests that Dicer is essential for the repression of periportal proteins achieved by active Wnt signalling and that Dicer may act downstream of β-catenin/TCF. However, *Dicer1* expression was not affected in β-catenin-deficient livers, indicating that *Dicer1* itself is not involved immediately downstream of Wnt signalling (Figure 4A).

Furthermore, we performed a microarray analysis to test whether individual microRNAs are regulated by β-catenin. Similarly, a comparison of β-catenin-deficient and control livers identified no microRNAs whose expression levels were down-regulated in β-catenin-deficient livers. Thus, we did not find any microRNAs that were directly activated by β-catenin/TCF signalling (Figure 4B and Supporting information, Supplementary Table 1). On the other hand, the analysis identified four microRNAs that were up-regulated in β-catenin-deficient livers: miR-31 (2.84-fold), miR-34a (2.77-fold), miR-31* (2.91-fold), and miR-193b (2.21-fold). However, considering the modest increase

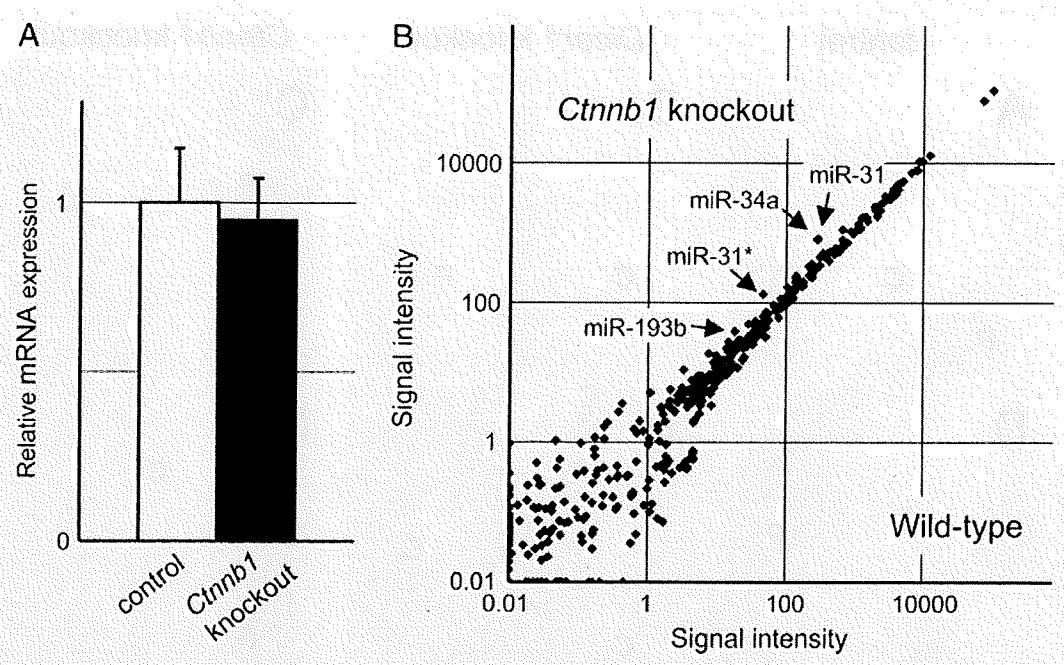

Figure 4. Expression of *Dicer1* and microRNAs in β-catenin-deficient liver. (A) Expression of *Dicer1* as determined using quantitative PCR ($n = 6$ per group). (B) Microarray analysis of microRNA expression ($n = 3$ per group). The four microRNAs with significantly altered expressions are indicated by the arrows

of these microRNAs, these changes are unlikely to explain the dramatically altered expression of periportal proteins.

In summary, our data demonstrate that neither the expression of *Dicer1* nor that of individual microRNAs is dependent on β-catenin/TCF signalling. Thus, while Dicer and β-catenin elimination results in similar defects with regard to the inappropriate expression of periportal proteins, our results indicate that Dicer and microRNA expression is not directly controlled by Wnt signalling.

Discussion

Recent studies have suggested that the Wnt/β-catenin/TCF signalling pathway plays a key role in the establishment of liver zonation [4,5]. As observations of β-catenin-deficient liver have indicated, β-catenin-mediated signalling is essential for both the expression of pericentral proteins and the repression of periportal proteins in pericentral hepatocytes. Even though MAPK signalling has been reported to affect zonation through the modulation of β-catenin/TCF-dependent transcription [11], the mechanisms underlying the establishment of zonation remain largely undefined. The present study identified Dicer as a novel and essential component in the establishment of one aspect of liver zonation, the repression of periportal proteins in pericentral areas.

The hepatocyte-specific loss of Dicer resulted in the diffuse expression of proteins that are normally localized to the periportal areas. On the other hand, the localization of pericentral proteins was left mostly unaltered. Since pericentral protein expression requires active Wnt signalling [4,8,9], the conservation of pericentral protein expression in Dicer-deficient livers indicates that the loss of Dicer does not affect Wnt activity in pericentral hepatocytes. In contrast, our findings in Dicer-deficient livers suggest that the repression of periportal proteins by active Wnt signalling requires Dicer. While the induction of pericentral proteins and the repression of periportal proteins are coordinated by Wnt signalling, these processes are regulated independently of each other, and Dicer is selectively required for the repression of periportal proteins.

To explore how Dicer is involved in the repression of periportal proteins, we first tested whether the expression of Dicer itself was regulated by β-catenin/TCF; however, the expression of *Dicer1* was not altered in β-catenin-deficient livers. The primary physiological role of Dicer is microRNA processing [12,19]. While Dicer has microRNA-independent functions, such as endogenous siRNA processing in at least some organs [20,21], Dicer's functions are generally thought to be largely mediated by microRNAs. Since microRNA precursors are mostly transcribed by RNA polymerase II [22], some microRNAs might be transactivated by β-catenin/TCF, resulting in suppression of periportal genes. Nevertheless, we could not identify any microRNAs that were down-regulated in β-catenin-deficient livers. Collectively, these observations imply that Dicer plays an essential role in the repression of periportal proteins at some point downstream of β-catenin/TCF signalling, albeit this effect likely occurs through an indirect mechanism.

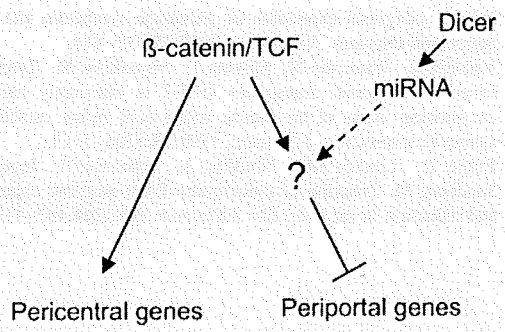

Figure 5. Model of the regulation of zonal gene expression. β-Catenin/TCF transactivates pericentral genes as well as represses periportal genes. Dicer and microRNAs are essential for the repression of periportal genes, but are not directly regulated by β-catenin

The disruption of Dicer did not have a major effect on the localization of pericentral proteins, but it did result in the expression of GS in a broader area. This finding indicates that a suppressive signal mediated by Dicer is required for the repression of GS in distal pericentral areas. A previous study reported that loss of Hnf4a also caused aberrant GS expression [23]. However, the loss of Hnf4a resulted in weak expression of GS in the entire lobule, unlike in Dicer-deficient livers, and the expression of Hnf4a was not altered in Dicer-deficient livers [18]. While the loss of Dicer and Hnf4a both affected the localization of GS, these two molecules seem to regulate GS expression through independent mechanisms.

In summary, the present study shows that Dicer is required for the establishment of proper liver zonation. Dicer is essential for the suppression of periportal proteins by Wnt/β-catenin/TCF signalling, albeit neither Dicer itself nor any individual microRNAs are directly activated by β-catenin/TCF. Our results suggest that Dicer regulates factor(s) that suppress periportal genes at some point downstream of β-catenin (Figure 5). However, the individual microRNAs responsible for the repression of periportal proteins remain elusive at present. Further studies of individual microRNAs should help to elucidate the precise mechanisms by which these factors regulate zonal gene expression in the liver.

Acknowledgements

We thank Ms Kaho Minoura (Agilent Technologies) for the microRNA analysis, Dr Magnus Ingelman-Sundberg (Karolinska Institute, Stockholm, Sweden) and Dr Masahiko Watanabe (Hokkaido University, Sapporo, Japan) for providing antibodies, and Mr Shigeru Tamura for photographic assistance. This work was supported by KAKENHI (20790315) from the Ministry of Education, Culture, Sports, Science and Technology, Japan, and a Grant-in-Aid for the Third Term Comprehensive 10-Year Strategy for Cancer Control and a Grant-in-Aid for Cancer Research from the Ministry of Health, Labour, and Welfare of Japan. Work in MH's laboratory was supported by a NIH grant (CA112537).

References

1. Jungermann K, Kietzmann T. Zonation of parenchymal and nonparenchymal metabolism in liver. *Annu Rev Nutr* 1996;**16:**179–203.
2. Gebhardt R. Metabolic zonation of the liver: regulation and implications for liver function. *Pharmacol Ther* 1992;**53:**275–354.
3. Braeuning A, Ittrich C, Kohle C, Hailfinger S, Bonin M, Buchmann A, *et al.* Differential gene expression in periportal and perivenous mouse hepatocytes. *FEBS J* 2006;**273:**5051–5061.
4. Benhamouche S, Decaens T, Godard C, Chambrey R, Rickman DS, Moinard C, *et al.* Apc tumor suppressor gene is the 'zonation-keeper' of mouse liver. *Dev Cell* 2006;**10:**759–770.
5. Hailfinger S, Jaworski M, Braeuning A, Buchmann A, Schwarz M. Zonal gene expression in murine liver: lessons from tumors. *Hepatology* 2006;**43:**407–414.
6. Gordon MD, Nusse R. Wnt signaling: multiple pathways, multiple receptors, and multiple transcription factors. *J Biol Chem* 2006;**281:**22429–22433.
7. Sekine S, Gutierrez P, Lan B, Feng S, Hebrok M. Liver specific loss of beta-catenin results in delayed hepatocyte proliferation after partial hepatectomy. *Hepatology* 2007;**45:**361–368.
8. Colnot S, Decaens T, Niwa-Kawakita M, Godard C, Hamard G, Kahn A, *et al.* Liver-targeted disruption of Apc in mice activates beta-catenin signaling and leads to hepatocellular carcinomas. *Proc Natl Acad Sci U S A* 2004;**101:**17216–17221.
9. Sekine S, Lan BY, Bedolli M, Feng S, Hebrok M. Liver-specific loss of beta-catenin blocks glutamine synthesis pathway activity and cytochrome p450 expression in mice. *Hepatology* 2006;**43:**817–825.
10. Braeuning A, Ittrich C, Koehle C, Buchmann A, Schwarz M. Zonal gene expression in mouse liver resembles expression patterns of Ha-ras and {beta}-catenin mutated hepatomas. *Drug Metab Dispos* 2007;**35:**503–507.
11. Braeuning A, Menzel M, Kleinschnitz EM, Harada N, Tamai Y, Kohle C, *et al.* Serum components and activated Ha-ras antagonize expression of perivenous marker genes stimulated by beta-catenin signaling in mouse hepatocytes. *FEBS J* 2007;**274:**4766–4777.
12. Harfe BD, McManus MT, Mansfield JH, Hornstein E, Tabin CJ. The RNaseIII enzyme Dicer is required for morphogenesis but not patterning of the vertebrate limb. *Proc Natl Acad Sci U S A* 2005;**102:**10898–10903.
13. Murchison EP, Partridge JF, Tam OH, Cheloufi S, Hannon GJ. Characterization of Dicer-deficient murine embryonic stem cells. *Proc Natl Acad Sci U S A* 2005;**102:**12135–12140.
14. Kanellopoulou C, Muljo SA, Kung AL, Ganesan S, Drapkin R, Jenuwein T, *et al.* Dicer-deficient mouse embryonic stem cells are defective in differentiation and centromeric silencing. *Genes Dev* 2005;**19:**489–501.
15. Postic C, Shiota M, Niswender KD, Jetton TL, Chen Y, Moates JM, *et al.* Dual roles for glucokinase in glucose homeostasis as determined by liver and pancreatic beta cell-specific gene knock-outs using Cre recombinase. *J Biol Chem* 1999;**274:**305–315.
16. Postic C, Magnuson MA. DNA excision in liver by an albumin-Cre transgene occurs progressively with age. *Genesis* 2000;**26:**149–150.
17. Brault V, Moore R, Kutsch S, Ishibashi M, Rowitch DH, McMahon AP, *et al.* Inactivation of the beta-catenin gene by Wnt1-Cre-mediated deletion results in dramatic brain malformation and failure of craniofacial development. *Development* 2001;**128:**1253–1264.
18. Sekine S, Ogawa R, Ito R, Hiraoka N, McManus MT, Kanai Y, *et al.* Disruption of Dicer1 induces dysregulated fetal gene expression and promotes hepatocarcinogenesis. *Gastroenterology* 2009;**136:**2304–2315.
19. Calabrese JM, Seila AC, Yeo GW, Sharp PA. RNA sequence analysis defines Dicer's role in mouse embryonic stem cells. *Proc Natl Acad Sci U S A* 2007;**104:**18097–18102.
20. Tam OH, Aravin AA, Stein P, Girard A, Murchison EP, Cheloufi S, *et al.* Pseudogene-derived small interfering RNAs regulate gene expression in mouse oocytes. *Nature* 2008;**453:**534–538.

21. Watanabe T, Totoki Y, Toyoda A, Kaneda M, Kuramochi-Miyagawa S, Obata Y, *et al.* Endogenous siRNAs from naturally formed dsRNAs regulate transcripts in mouse oocytes. *Nature* 2008;**453:**539–543.
22. Lee Y, Kim M, Han J, Yeom KH, Lee S, Baek SH, *et al.* MicroRNA genes are transcribed by RNA polymerase II. *EMBO J* 2004;**23:**4051–4060.
23. Stanulovic VS, Kyrmizi I, Kruithof-de Julio M, Hoogenkamp M, Vermeulen JL, Ruijter JM, *et al.* Hepatic HNF4alpha deficiency induces periportal expression of glutamine synthetase and other pericentral enzymes. *Hepatology* 2007;**45:**433–444.
24. Yamada K, Watanabe M, Shibata T, Nagashima M, Tanaka K, Inoue Y. Glutamate transporter GLT-1 is transiently localized on growing axons of the mouse spinal cord before establishing astrocytic expression. *J Neurosci* 1998;**18:**5706–5713.
25. Buhler R, Lindros KO, Nordling A, Johansson I, Ingelman-Sundberg M. Zonation of cytochrome P450 isozyme expression and induction in rat liver. *Eur J Biochem* 1992;**204:**407–412.

SUPPORTING INFORMATION ON THE INTERNET

The following supporting information may be found in the online version of this article.

Table S1. MicroRNA expression in β-catenin-deficient liver

J Pathol 2009; **219**: 365–372 DOI: 10.1002/path

Virchows Arch (2009) 454:513–517
DOI 10.1007/s00428-009-0762-6

ORIGINAL ARTICLE

Esophageal melanomas harbor frequent *NRAS* mutations unlike melanomas of other mucosal sites

Shigeki Sekine · Yukihiro Nakanishi · Reiko Ogawa · Satoko Kouda · Yae Kanai

Received: 4 January 2009 / Revised: 26 February 2009 / Accepted: 8 March 2009 / Published online: 25 March 2009

Abstract Mucosal melanomas have genetic alterations distinct from those in cutaneous melanomas. For example, *NRAS*- and *BRAF*-activating mutations occur frequently in cutaneous melanomas, but not in mucosal melanomas. We examined 16 esophageal melanomas for genetic alterations in *NRAS*, *BRAF*, and *KIT* to determine whether they exhibit genetic features common to melanomas arising from other mucosal sites. A sequencing analysis identified *NRAS* mutations in six cases; notably, four of these mutations were located in exon 1, an uncommon mutation site in cutaneous and other mucosal melanomas. *BRAF* and *KIT* mutations were found in one case each. Immunohistochemistry showed KIT expression in four cases, including the tumor with a *KIT* mutation and two other intramucosal tumors. The low frequency of *BRAF* mutations and the presence of a *KIT* mutation-positive case are findings similar to those of mucosal melanomas of other sites, but the prevalence of *NRAS* mutations was even higher than that of cutaneous melanomas. The present study implies that esophageal melanomas have genetic alterations unique from those observed in other mucosal melanomas.

Keywords *NRAS* · *BRAF* · *KIT* · Esophageal melanoma

Introduction

Melanomas show distinct patterns of genetic alterations depending on their sites of origin. The anatomical site-specific patterns of genetic alterations have been discussed in relation to the extent of ultraviolet exposure. *NRAS* and *BRAF* are the most frequently mutated oncogenes in melanomas. Both mutant N-Ras and B-Raf promote tumorigenesis through the constitutive activation of the MAP kinase pathway. Earlier studies suggested that *NRAS* mutations were frequent among melanomas arising from sun-exposed skin [1, 2]. Subsequently, *BRAF*-activating mutations were also identified in a significant proportion of melanomas [3]. Curtin et al. analyzed *NRAS* and *BRAF* mutations as well as DNA copy number changes in a large cohort of melanomas [4]. They utilized the presence of solar elastosis as a histological hallmark of chronic sun exposure and indicated that the majority of melanomas occurring on skin without chronic sun-induced damage had either *NRAS* or *BRAF* mutations whereas melanomas arising on skin with chronic sun-induced damage, acral sites, and mucosal membranes had mostly wild-type *NRAS* and *BRAF*. At the same time, they demonstrated that each group of melanomas exhibited distinct patterns of DNA copy number changes.

In addition to *NRAS* and *BRAF* mutations, a subset of melanomas contains *KIT* mutations [5–7]. Remarkably, the prevalence of *KIT* mutations also varies depending on the site of tumor origin, with the highest prevalence observed in mucosal melanomas [5]. Thus, genetic alterations in melanomas show site/organ-specific patterns and mucosal melanomas have distinct genetic features from those of cutaneous melanomas.

Esophageal melanomas are exceedingly rare, but highly aggressive neoplasms [8–10]. Previous studies have reported that melanomas constitute only 0.1–0.3% of all esophageal tumors [11, 12]. The rarity of this tumor is reasonable, considering the fact that the esophagus usually lacks melanocytes [13]. In addition, the esophagus is not

S. Sekine · Y. Nakanishi · R. Ogawa · S. Kouda · Y. Kanai (✉)
Pathology Division, National Cancer Center Research Institute,
5-1-1, Tsukiji, Chuo-ku,
Tokyo, Japan
e-mail: ykanai@ncc.go.jp

exposed to ultraviolet radiation, a major risk factor for melanomas. Because of the rarity of this lesion, data on genetic alterations in esophageal melanomas is scarce. However, the characterization of their genetic features, including how they differ from cutaneous melanomas and melanomas of other mucosal sites would contribute to the understanding of site/organ-specific genetic alterations in melanomas. Furthermore, considering the development of specific kinase inhibitors, such information could be critical for choosing an appropriate treatment. In this paper, we present the results of a mutational analysis of *NRAS*, *BRAF*, and *KIT* in 16 cases of esophageal melanomas.

Materials and methods

Sixteen surgically resected esophageal melanomas were examined in the present study (Table 1). The samples were routinely fixed with 10% formalin and embedded in paraffin. Five-micrometer-thick sections of each specimen were stained briefly with hematoxylin and eosin and used for DNA extraction. The tumor and nontumor areas were separately dissected using sterilized toothpicks under a microscope. Tissues obtained from the proper muscle layer distant from the tumors were used as nontumor samples. The dissected samples were incubated in 100 μL of DNA extraction buffer (50 mmol/L Tris–HCl, pH 8.0, 1 mmol/L ethylenediaminetetraacetic acid, 0.5% (*v*/*v*) Tween 20, 200 μg/mL proteinase K) at 37°C overnight. Proteinase K was inactivated by heating at 100°C for 10 min. The DNA samples were subjected to polymerase chain reaction (PCR) directly or after purification. When required, the samples were purified using a QIAquick PCR Purification Kit (Qiagen, Hilden, Germany). PCR was performed for 3 min at 95°C for initial denaturing, followed by 35 or 40 cycles at 94°C for 15 s, 58°C for 20 s, and 72°C for 60 s and a final extension at 72°C for 5 min. The primers that were used are listed in Table 2. The PCR products were electrophoresed in a 2% (*w*/*v*) agarose gel, visualized under UV light with ethidium bromide staining, and recovered using a QIAquick Gel Extraction Kit (Qiagen). Isolated PCR products were sequenced bidirectionally on an Applied Biosystems 3130 Genetic Analyzer (Applied Biosystems, Foster, CA, USA) using the same primers used for amplification. Each experiment, including DNA extraction, was done at least twice.

Immunohistochemical staining was performed using the avidin–biotin complex method. The primary antibody used was polyclonal anti-KIT (A4502; 1:100 dilution; Dako, Denmark). 3-3′-Diaminobenzidine tetrahydrochloride was used as a chromogen. The sections were counterstained with hematoxylin. Mast cells in the sections were used as positive controls. For negative controls, the tissue was processed in the same way but the primary antibody was omitted. The staining

Table 1 Results of mutational analysis and immunohistochemistry

Case no.	Age/sex	Depth of invasion	*BRAF*		*NRAS*		*KIT*		KIT IHC
			Nucleotide	Amino acid	Nucleotide	Amino acid	Nucleotide	Amino acid	
1	62/M	Mucosa	–		–		–		+++ (membranous)
2	67/M	Mucosa	–		–		–		+++ (membranous)
3	48/M	Submucosa	–		–		–		–
4	57/F	Submucosa	–		A183T	Q61H	–		–
5	64/M	Submucosa	–		–		–		–
6	67/M	Submucosa	–		–		–		–
7	72/M	Submucosa	–		G35C	G12A	–		–
8	73/M	Submucosa	–		–		–		–
9	48/M	Muscularis propria	–		–		C1727T	L576P	+++ (cytoplasmic)
10	68/M	Muscularis propria	T1799A	V600E	–		–		–
11	69/M	Muscularis propria	–		G34C	G12R	–		–
12	70/M	Muscularis propria	–		G38C	G13A	–		–
13	63/M	Adventitia	–		A183T	Q61H	–		–
14	64/M	Adventitia	–		–		–		–
15	68/M	Adventitia	–		G37C	G13R	–		–
16	71/M	Adventitia	–		–		–		++ (membranous)

IHC immunohistochemistry

Table 2 Primers used in the present study

	Forward primer	Reverse primer
BRAF exon15	TGTTTGCTCTGATAGGAAAATG	CTGATGGGACCCACTCCAT
NRAS exon 1	CAGGTTCTTGCTGGTGTGAAATGACTGAG	CTACCACTGGGCCTCACCTCTATGG
NRAS exon 2	AACAAGTGGTTATAGATGGTGA	CGTTAGAGGTTAATATCCGCA
KIT exon 11	TTTCCCTTTCTCCCCACAG	AAAGCCCCTGTTTCATACTGAC
KIT exon 13	TGCTAAAATGCATGTTTCCAAT	CAGCTTGGACACGGCTTTAC
KIT exon 17	TTTCTTTTCTCCTCCAACCTAA	TGTCAAGCAGAGAATGGGTACT

results were evaluated based on the amount of immunopositive tumor cells as follows: − [<5%], + [5–25%], ++ [25–75%], +++ [>75%]. When KIT is expressed, the staining intensity and the subcellular localization were also evaluated.

Results

The results of the mutational analysis are summarized in Table 1. A *BRAF* mutation was found in one case, while *NRAS* mutations were observed in six cases (Fig. 1). Four of six *NRAS* mutations were located in exon 1, and all these mutations were G to C transversions. All *BRAF* and *NRAS* mutations were missense mutations that had been previously identified as being oncogenic. A missense *KIT* mutation was observed in one case. The mutation affected the juxtamembrane domain of KIT. The wild-type sequence signal was very low for this mutation, suggesting that it was a homozygous mutation. All samples from nontumor areas showed wild-type sequences, indicating the somatic nature of the mutations. All the mutations that were observed were mutually exclusive.

Immunohistochemistry showed no or only focal and equivocal KIT expression in 12 cases (Fig. 2a). The case with the *KIT* mutation showed strong cytoplasmic expression (Fig. 2b), and another case showed heterogeneous staining with approximately 70% of the area exhibiting moderate membranous expression (Fig. 2c). Based on the heterogeneous KIT expression, we performed an additional mutational analysis. The KIT-positive and KIT-negative areas were separately subjected to sequencing analysis, but no *KIT* mutations were observed in either sample. Two early-stage melanomas limited to the mucosal layer exhibited strong and diffuse membranous KIT expression (Fig. 2d).

Discussion

NRAS and *BRAF* mutations are the most common genetic alterations in melanomas. An extensive literature review by Hocker and Tsao reported overall mutation rates of 26% for *NRAS* and 42% for *BRAF* in cutaneous melanomas [14]. In contrast, several studies concurred that these mutations are significantly less prevalent in mucosal melanomas with reported frequencies of 5–14% for *NRAS* and 0–10% for *BRAF* [2, 4, 15–17].

Our results showed that *BRAF* mutations are uncommon among esophageal melanomas as in mucosal melanomas of other organs. Unexpectedly, however, six of the 16 melanomas were found to harbor *NRAS*-activating mutations. While our series may not be sufficiently large to determine the mutational frequency conclusively, the prevalence of *NRAS* mutation-positive cases in the present series was even higher than that observed in cutaneous melanomas. Notably, four of the six mutations were located in exon 1 of *NRAS* and all these mutations were G to C transversions. This finding is intriguing as *NRAS* mutations in melanomas predominantly affect codon 61 within exon 2 and G to C transversion is a rare type of mutations for these sites [14].

Furthermore, previous studies showed that a few recurrent mutations are responsible for the vast majority of *NRAS* mutations in melanomas. The literature review by Hocker and Tsao showed that three mutations, G35A, C181A, and A182G, accounted for 82% of *NRAS* mutations of the 255 substitutions at the *NRAS* locus [14]. However, surprisingly, none of the six mutations identified in this study were identical to these most common *NRAS* mutations. These observations suggest that esophageal melanomas have a high frequency of *NRAS* mutations with a unique mutation spectrum.

Our literature review identified only one study analyzing *NRAS* and *BRAF* mutations in esophageal melanomas. Wong et al. examined three cases of esophageal melanomas, two of which had *NRAS*-activating mutations affecting codons 12 and 61, respectively [17]. On the other hand, only two *BRAF* and three *NRAS* mutations were identified in 33 mucosal melanomas arising outside of the esophagus in their series. While the number of subjects in their study was small, their result is consistent with our finding that esophageal melanomas have a high prevalence of *NRAS* mutations.

A *KIT* mutation was identified in one case, indicating that a subset of esophageal melanomas harbor *KIT*-activating mutations as in other mucosal melanomas. An identical mutation has been reported in gastrointestinal

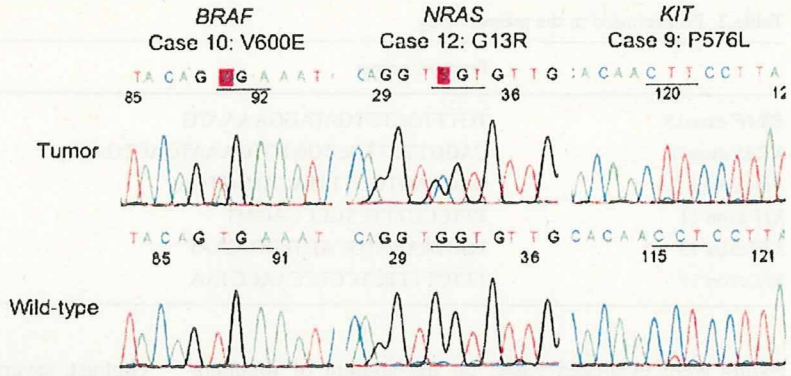

Fig. 1 Representative mutations of *BRAF*, *NRAS*, and *KIT* in esophageal melanomas. Heterozygous *BRAF* V600E and *NRAS* G13R mutations and homozygous P576L *KIT* mutation are shown

stromal tumors and anal melanomas [7, 18], and this mutation has been shown to be associated with a sensitivity to dasatinib and imatinib, inhibitors of SRC/ABL and KIT [7]. While the frequency of this mutation was not high in the present series, the identification of a *KIT* mutation is important, since it provides an immediate therapeutic application. Indeed, the successful treatments of melanomas with *KIT* mutations by imatinib have been recently reported [19, 20].

Of note, the case with the *KIT* mutation also exhibited the strong expression of KIT protein, whereas the majority of the mutation-negative melanomas did not express KIT, as determined using immunohistochemistry. This finding agrees with the results of previous studies on mucosal melanomas of other sites and suggests that immunohistochemistry is useful for excluding *KIT* mutation-negative cases prior to genetic testing [6, 7]. We also found KIT expression in two early-stage tumors. The expression of KIT in early-stage cutaneous melanomas has also been previously reported [21, 22]. Since non-neoplastic melanocytes express KIT, the expression of KIT in early-stage melanomas might be regarded as the retention of physiological expression in melanocytes [21]. Overall, our observations suggest that immunohistochemistry for KIT may be useful for prescreening *KIT* mutation-positive cases among advanced esophageal melanomas.

The present study indicates that esophageal melanomas have a high frequency of *NRAS* mutations unlike mucosal melanomas of other sites. Furthermore, the mutational spectrum of *NRAS* is distinct from those commonly observed in melanomas. Even among mucosal melanomas, the patterns of genetic alterations are likely distinct between

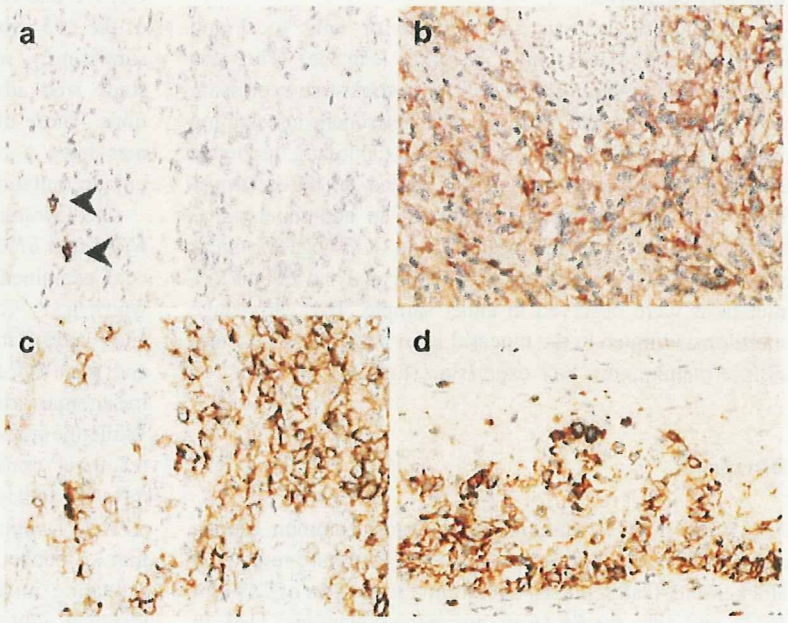

Fig. 2 KIT expression in esophageal melanomas. **a** This case lacks KIT expression. Few mast cells show positive staining (*arrowheads*; case 13). **b** Tumor cells show diffuse cytoplasmic staining (case 9). **c** An area of the tumor cells shows membranous expression (case 16). **d** Tumor cells proliferating within the epithelial layer show membranous expression (case 2)

differing sites of origin. Our observations also suggest that not only the degree of ultraviolet exposure, but also organ-specific factors may significantly influence the mutational spectrum in melanomas.

Acknowledgements This work was supported by a Grant-in-Aid for the Third Term Comprehensive 10-Year Strategy for Cancer Control, a Grant-in-Aid for Cancer Research from the Ministry of Health, Labor and Welfare of Japan, and a program for promotion of Fundamental Studies in Health Sciences of the National Institute of Biomedical Innovation (NiBio), Japan.

Conflicts of interest The authors declare that they have no conflicts of interest.

References

1. van't Veer LJ, Burgering BM, Versteeg R et al (1989) N-ras mutations in human cutaneous melanoma from sun-exposed body sites. Mol Cell Biol 9:3114–3116
2. Jiveskog S, Ragnarsson-Olding B, Platz A et al (1998) N-ras mutations are common in melanomas from sun-exposed skin of humans but rare in mucosal membranes or unexposed skin. J Invest Dermatol 111:757–761
3. Davies H, Bignell GR, Cox C et al (2002) Mutations of the BRAF gene in human cancer. Nature 417:949–954
4. Curtin JA, Fridlyand J, Kageshita T et al (2005) Distinct sets of genetic alterations in melanoma. N Engl J Med 353:2135–2147
5. Curtin JA, Busam K, Pinkel D et al (2006) Somatic activation of KIT in distinct subtypes of melanoma. J Clin Oncol 24:4340–4346
6. Rivera RS, Nagatsuka H, Gunduz M et al (2008) C-*kit* protein expression correlated with activating mutations in KIT gene in oral mucosal melanoma. Virchows Arch 452:27–32
7. Antonescu CR, Busam KJ, Francone TD et al (2007) L576P KIT mutation in anal melanomas correlates with KIT protein expression and is sensitive to specific kinase inhibition. Int J Cancer 121:257–264
8. Kato H, Watanabe H, Tachimori Y et al (1991) Primary malignant melanoma of the esophagus: report of four cases. Jpn J Clin Oncol 21:306–313
9. Li B, Lei W, Shao K et al (2007) Characteristics and prognosis of primary malignant melanoma of the esophagus. Melanoma Res 17:239–242
10. Lohmann CM, Hwu WJ, Iversen K et al (2003) Primary malignant melanoma of the oesophagus: a clinical and pathological study with emphasis on the immunophenotype of the tumours for melanocyte differentiation markers and cancer/testis antigens. Melanoma Res 13:595–601
11. Turnbull AD, Rosen P, Goodner JT et al (1973) Primary malignant tumors of the esophagus other than typical epidermoid carcinoma. Ann Thorac Surg 15:463–473
12. Scotto J, Fraumeni JF Jr, Lee JA (1976) Melanomas of the eye and other noncutaneous sites: epidemiologic aspects. J Natl Cancer Inst 56:489–491
13. Tateishi R, Taniguchi H, Wada A et al (1974) Argyrophil cells and melanocytes in esophageal mucosa. Arch Pathol 98:87–89
14. Hocker T, Tsao H (2007) Ultraviolet radiation and melanoma: a systematic review and analysis of reported sequence variants. Hum Mutat 28:578–588
15. Cohen Y, Rosenbaum E, Begum S et al (2004) Exon 15 BRAF mutations are uncommon in melanomas arising in nonsun-exposed sites. Clin Cancer Res 10:3444–3447
16. Edwards RH, Ward MR, Wu H et al (2004) Absence of BRAF mutations in UV-protected mucosal melanomas. J Med Genet 41:270–272
17. Wong CW, Fan YS, Chan TL et al (2005) BRAF and NRAS mutations are uncommon in melanomas arising in diverse internal organs. J Clin Pathol 58:640–644
18. Lasota J, Jasinski M, Sarlomo-Rikala M et al (1999) Mutations in exon 11 of c-*Kit* occur preferentially in malignant versus benign gastrointestinal stromal tumors and do not occur in leiomyomas or leiomyosarcomas. Am J Pathol 154:53–60
19. Hodi FS, Friedlander P, Corless CL et al (2008) Major response to imatinib mesylate in KIT-mutated melanoma. J Clin Oncol 26:2046–2051
20. Lutzky J, Bauer J, Bastian BC (2008) Dose-dependent, complete response to imatinib of a metastatic mucosal melanoma with a K642E KIT mutation. Pigment Cell Melanoma Res 21:492–493
21. Montone KT, van Belle P, Elenitsas R et al (1997) Proto-oncogene c-*kit* expression in malignant melanoma: protein loss with tumor progression. Mod Pathol 10:939–944
22. Janku F, Novotny J, Julis I et al (2005) KIT receptor is expressed in more than 50% of early-stage malignant melanoma: a retrospective study of 261 patients. Melanoma Res 15:251–256

CME/SAM

Prognostic Significance of CXCL12 Expression in Patients With Colorectal Carcinoma

Yuri Akishima-Fukasawa, MD, PhD,[1] Yukihiro Nakanishi, MD, PhD,[1] Yoshinori Ino,[1] Yoshihiro Moriya, MD, PhD,[2] Yae Kanai, MD, PhD,[1] and Setsuo Hirohashi, MD, PhD[1]

Key Words: CXCL12; Invasive front; Immunohistochemistry; Colorectal carcinoma; Prognosis

DOI: 10.1309/AJCPK35VZJEWCUTL

Upon completion of this activity you will be able to:
- define the World Health Organization criteria for the histologic grading of the differentiation of colorectal carcinoma.
- discuss the role of examination of the invasive front of colorectal carcinoma for tumor budding and how this may pertain to prognosis.
- discuss the potential application of immunohistochemical staining for CXCL12 to highlight tumor budding in colorectal carcinoma.

The ASCP is accredited by the Accreditation Council for Continuing Medical Education to provide continuing medical education for physicians. The ASCP designates this educational activity for a maximum of 1 *AMA PRA Category 1 Credit* ™ per article. This activity qualifies as an American Board of Pathology Maintenance of Certification Part II Self-Assessment Module.

The authors of this article and the planning committee members and staff have no relevant financial relationships with commercial interests to disclose.

Questions appear on p 307. Exam is located at www.ascp.org/ajcpcme.

Abstract

The present study investigated the protein expression level of CXCL12 in colorectal cancer and aimed to elucidate its association with prognosis. CXCL12 positivity in 50% or more of tumor cells was defined as high expression and that in less than 50% of the tumor cells as low expression. CXCL12+ tumor budding at the invasive front was divided into 2 grades: high with 10 or more budding foci per ×200 field of view and low grade with fewer than 10 budding foci. Patients with high expression (72.7%) and high grade CXCL12+ tumor budding (43.0%) had significantly shorter survival than patients with low expression (P = .014) and low grade (P = .003), respectively. Patients with a combination of high expression and high grade had the worst outcome (P < .001). Our study demonstrated that CXCL12 expression in colorectal cancer cells and at sites of budding were significant prognostic factors. Furthermore, together with lymph node metastasis, a combination of both expression patterns was a more powerful independent prognostic factor.

Several studies have revealed that the establishment of metastasis is the final outcome of a series of phenomena including tumor cell deposition in distant organs, clonogenic growth, and angiogenesis. These processes are fundamental for tumor cell survival and tumor metastasis and are regulated by interactions of cancer cells with the host microenvironment.[1-3] The CXC chemokine ligand-12 (CXCL12), stromal cell derived factor-1, is a member of the CXC chemokine family, which has been initially cloned from murine bone marrow and characterized as a pre B-cell growth-stimulating factor.[4-6] CXCL12 exerts effects through its physiologic cognate receptor, CXC chemokine receptor 4 (CXCR4), and is known to have roles in chemotaxis,[7] hematopoiesis,[8] and angiogenesis.[9,10] In addition, CXCR4 is involved in tumor cell homing to specific organs and in tumor progression.[11-13] CXCL12/CXCR4 also has a critical role in determining the metastatic destination of breast cancer cells.[12] It is also evident that some CXCR4+ tumors, including colorectal cancer,[1,13,14] exhibit marked malignant behavior.[12,15,16] So far, few studies have focused on chemokine expression in cancer cells,[17-21] and little is known about the clinicopathologic significance of CXCL12 expression in patients with colorectal cancer.

In this study, we attempted to evaluate the clinicopathologic significance of CXCL12 expression in patients with colorectal cancer by using immunohistochemical analysis together with examination of conventional histopathologic features.

Materials and Methods

Between 1996 and 1997 at the National Cancer Center Hospital, Tokyo, Japan, 165 patients underwent surgery for primary colorectal carcinoma, including 100 colon (60.6%)

and 65 rectal (39.4%) cancers. Sample selection was restricted to consecutive cases diagnosed as stages II and III according to the International Union Against Cancer TNM classification.[22] Of the 165 cases, 72 (43.6%) were classified as stage II and 93 (56.4%) as stage III; 116 cases (70.3%) were T2-3, and 49 were T4 (29.7%).

All patients underwent curative resection, defined as the removal of gross cancer and the demonstration of tumor-negative surgical margins by histopathologic examination of the total circumference. No patients received preoperative chemotherapy, and all patients were free of distant visceral metastases. The patients comprised 101 men and 64 women, ranging in age from 32 to 93 years (mean – SD, 61.8 – 11.2 years). Postsurgical follow-up studies were completed for all patients, with follow-up periods ranging from 3 to 2,544 days (median, 1,844 days). Postsurgical recurrence was diagnosed by ultrasonography and computed tomography. This study was approved by the National Cancer Center Ethics Committee, Tokyo, Japan.

All available routinely processed, formalin-fixed, and paraffin-embedded blocks of colorectal carcinoma were obtained. Sections containing the maximum diameter of the tumor were used in the present study. Age, sex, tumor location, tumor size, macroscopic type, depth of tumor invasion, tumor differentiation, tumor budding grade by H&E staining, lymphatic vessel invasion, blood vessel invasion, lymph node metastasis, liver metastasis, and lung metastasis were subjected to statistical analyses **Table 1**.

The grade of tumor differentiation was decided on the basis of the predominant component in the tumor according to the World Health Organization classification: the percentage of the tumor showing formation of gland-like structures can be used to define the grade; well differentiated (grade 1) lesions exhibit glandular structures in more than 95% of the tumor; moderately differentiated (grade 2) adenocarcinoma has 50% to 90% glands; poorly differentiated (grade 3) adenocarcinoma has 5% to 50%; and undifferentiated (grade 4) carcinoma has less than 5%. Mucinous adenocarcinoma and signet-ring cell carcinoma, by convention, are considered poorly differentiated (grade 3).[23]

The existence of tumor budding at the invasive front was also evaluated. The invasive front in this study was defined as all regions of the border area between the primary tumor and interstitium in the submucosa, muscularis propria, subserosa, or nonperitonealized pericolonic/perirectal tissues. In accordance with previous studies, an isolated single cancer cell or a cluster composed of fewer than 5 cancer cells observed in the stroma of the actively invasive region was defined as a budding focus.[24-26] After reviewing the H&E-stained slides from each case, a field where the budding foci were most intense was selected. The number of budding foci was counted using a 20× microscope objective, giving a final magnification of ×200. A count ranging from 0 to 9 budding foci per field was designated as low grade and a count of 10 or more as high grade, in accordance with previous studies.[25,26]

Immunohistochemical Studies

After deparaffinization, all sections were pretreated in citrate buffer (10 mmol/L, pH 6.0) at 121 C for 10 minutes for antigen retrieval. Endogenous peroxidase was blocked with 0.3% hydrogen peroxide in methanol for 20 minutes. The sections were then incubated with anti-CXCL12/SDF-1 monoclonal antibody (0.5 ng/mL; R&D Systems, Minneapolis, MN) at 4 C overnight. The immunostained sections were washed with phosphate-buffered saline and processed with an EnVision+ kit (DakoCytomation, Carpinteria, CA) in accordance with the manufacturer s instructions. Immunoproducts were visualized by using diaminobenzidine tetrahydrochloride, and the sections were counterstained with hematoxylin. As an internal positive control for CXCL12 staining, the immunopositivity of normal colorectal epithelia adjacent to the tumors and endothelial cells of blood vessels was used. Intensity of positive staining in tumor cells that was the same as or more than that in normal colorectal epithelia was considered positive. Sections from each paraffin block were used as negative control samples by replacing the primary antibody with normal mouse immunoglobulin. After immunohistochemical analysis, the tumors were categorized according to the ratio and localization of immunopositive tumor cells in the sections containing the maximum tumor diameter.

We examined the relationship between the CXCL12 positivity rate in tumor cells and various clinicopathologic factors and found that a cutoff value of 50% was the most powerful discriminatory factor. Accordingly, a cutoff index of 50% was selected for our study. When the proportion of tumor cells positive for CXCL12 was 50% or more, the tumor was defined as showing high CXCL12 expression, whereas tumors in which fewer than 50% of the cells were positive were defined as showing low CXCL12 expression.

In addition, CXCL12 expression in foci of tumor budding at the invasive front was quantified and scored by the same method as for evaluation of tumor budding grade using H&E-stained sections. After scanning each CXCL12-immunostained slide, a field where immunopositivity in the budding foci was the most intense was selected, and the number of CXCL12+ budding foci was counted at ×200 magnification. For all histopathologic variables, each macroscopic record and microscopic slide was analyzed by 2 experienced pathologists (Y.A.-F. and Y.N.) to reach a consensus.

Statistical Analysis

The relationships between clinicopathologic characteristics and the number of immunopositive tumor cells were analyzed by variance tests when appropriate. The χ^2 test was

DOI: 10.1309/AJCPK35VZJEWCUTL

used to analyze variables such as sex, tumor location, depth of tumor invasion, tumor differentiation, tumor budding grade assessed by H&E staining, lymphatic vessel invasion, blood vessel invasion, lymph node metastasis, liver metastasis, and lung metastasis. The Student *t* test was used for statistical comparisons of variables such as age and tumor size, and the Mann-Whitney *U* test was applied to compare the variables of macroscopic type. Survival was measured from the date of surgery to the end of the follow-up period or death. Overall survival curves were determined by using the Kaplan-Meier method and were analyzed by using the log-rank test. Univariate and multivariate survival analysis was performed by using the Cox proportional hazards regression model with the StatView, version 5.0 software package (SAS Institute, Cary, NC), in a stepwise manner.

Results

Expression of CXCL12 in Colorectal Cancer

Immunoreactivity of CXCL12 was observed in the cell membrane and/or cytoplasm of tumor cells **Image 1A**. The endothelial cells of blood vessels and normal intestinal epithelia, especially in the middle to upper third portion of the crypt,

Table 1
Correlation of CXCL12 Expression With Clinicopathologic Features*

	CXCL12 Expression			CXCL12+ Tumor Budding Grade			CXCL12 Expression and Tumor Budding Grade		
Variable	Low (n = 45)	High (n = 120)	*P*	Low (n = 94)	High (n = 71)	*P*	Others (n = 99)	High Expression With High Grade (n = 66)	*P*
Age (y)	62.9 ± 12.7	61.4 ± 10.7	.319	61.9 ± 11.5	61.6 ± 11.0	.778	62.4 ± 11.5	60.9 ± 10.8	.346
Sex			.986			.192			.096
Male	27	74		53	48		55	46	
Female	18	46		41	23		44	20	
Tumor location			.525			.622			.625
Colon	25	75		59	41		62	38	
Rectum	20	45		35	30		37	28	
Maximum tumor diameter (cm)	4.7 ± 2.1	5.1 ± 1.9	.155	5.1 ± 2.1	4.7 ± 1.6	.232	5.0 ± 2.1	4.8 ± 1.6	.589
Macroscopic type†			.943			.256			.287
1	3	9		10	2		10	2	
2	42	109		84	67		89	62	
3	0	2		0	2		0	2	
4	0	0		0	0		0	0	
Tumor depth‡			.001			<.001			<.001
T2, T3	40	76		78	38		81	35	
T4	5	44		16	33		18	31	
Tumor differentiation§			>.999			>.999			>.999
Grade 1/2	44	116		91	69		96	64	
Grade 3/4	1	4		3	2		3	2	
Tumor budding grade (H&E staining)			.013			<.001			<.001
Low	36	69		78	27		80	25	
High	9	51		16	44		19	41	
Lymphatic vessel invasion			.984			.324			.559
Present	36	94		71	59		76	54	
Absent	9	26		23	12		23	12	
Blood vessel invasion			>.999			.096			.150
Present	29	79		56	52		60	48	
Absent	16	41		38	19		39	18	
Lymph node metastasis			.411			.003			.022
Present	29	67		45	51		50	46	
Absent	16	53		49	20		49	20	
Liver metastasis			.044			.101			.052
Present	1	18		7	12		7	12	
Absent	44	102		87	59		92	54	
Lung metastasis			.071			.030			.014
Present	1	16		5	12		5	12	
Absent	44	104		89	59		94	54	

* Data are given as number of cases or mean – SD. *P* values were calculated by using the Mann-Whitney *U* test for age and maximum tumor diameter, the Student *t* test for macroscopic type, and the χ^2 test for all others.
According to the World Health Organization classification: 1, polypoid; 2, ulcerating circumscribed; 3, ulcerating infiltrative; 4, diffusely infiltrative.
According to the International Union Against Cancer TNM classification: T2, tumor invades the muscularis propria; T3, tumor invades through the muscularis propria into the subserosa or into nonperitonealized pericolic or perirectal tissues; T4, tumor directly invades other organs or structures and/or perforates the visceral peritoneum.
According to the World Health Organization classification: grade 1, well-differentiated adenocarcinoma; grade 2, moderately differentiated adenocarcinoma; grade 3, poorly differentiated adenocarcinoma, mucinous adenocarcinoma, and signet-ring cell carcinoma; grade 4, undifferentiated carcinoma.

DOI: 10.1309/AJCPK35VZJEWCUTL

were also positive for CXCL12. In addition, fibroblasts adjacent to cancer cells, as well as normal areas, were weakly positive, but their expression was significantly weaker than that of tumor cells. CXCL12 staining was localized diffusely or patchily, and CXCL12 was often expressed in tumor buds at the invasive front **Image 1B**.

The mean – SD proportion of CXCL12+ tumor cells was 60.8% – 27.3%. Of the 165 cases, 120 (72.7%) exhibited immunopositivity in 50% or more of the cancer cells.

Patients whose tumors had high CXCL12 expression had significantly shorter survival than patients whose tumors had low CXCL12 expression ($P = .014$ and $P = .005$, overall and recurrence-free survival rates, respectively; log-rank test) **Figure 1**. The correlations between the percentage of CXCL12 immunopositivity and clinicopathologic findings are shown in Table 1. The percentage of CXCL12 immunopositivity was correlated with the depth of tumor invasion, tumor budding grade determined by H&E staining, and liver metastasis.

The results of univariate analysis using the Cox proportional hazards model are shown in **Table 2**. CXCL12 expression was found to be a significant prognostic factor for overall and recurrence-free survival, together with depth of tumor invasion, tumor budding grade by H&E staining, and lymph node metastasis. In addition, blood vessel invasion was found to be a significant predictive factor for recurrence, whereas lymphatic vessel invasion tended to be predictive of recurrence. Multivariate analysis using the Cox proportional hazards model revealed that the percentage of CXCL12 immunopositivity and lymph node metastasis were independent prognostic factors for overall and recurrence-free survival **Table 3**.

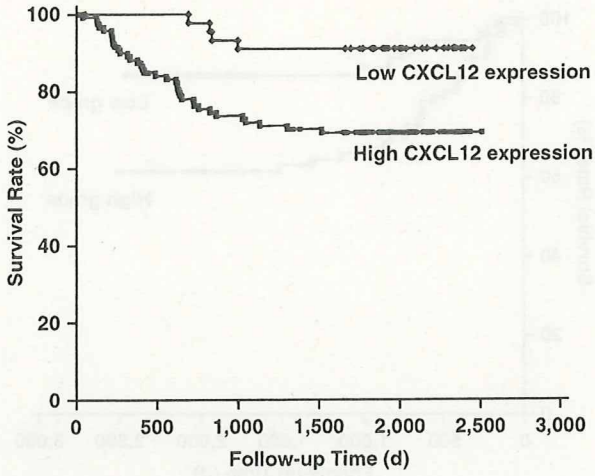

Figure 1 Kaplan-Meier survival curves of patients with colorectal carcinoma subdivided according to the proportion of tumor cells expressing CXCL12 ($P = .014$; log-rank test).

Grade of CXCL12 Immunopositivity in Foci of Tumor Budding

Of the 165 cases, 71 (43.0%) were defined as high grade, and the survival of the patients was significantly shorter than that of patients with low-grade tumors ($P = .003$ and $P < .001$, overall and recurrence-free survival rates, respectively; log-rank test) **Figure 2**. The number of CXCL12+ budding foci was correlated with the depth of tumor invasion ($P < .001$), tumor budding grade by H&E

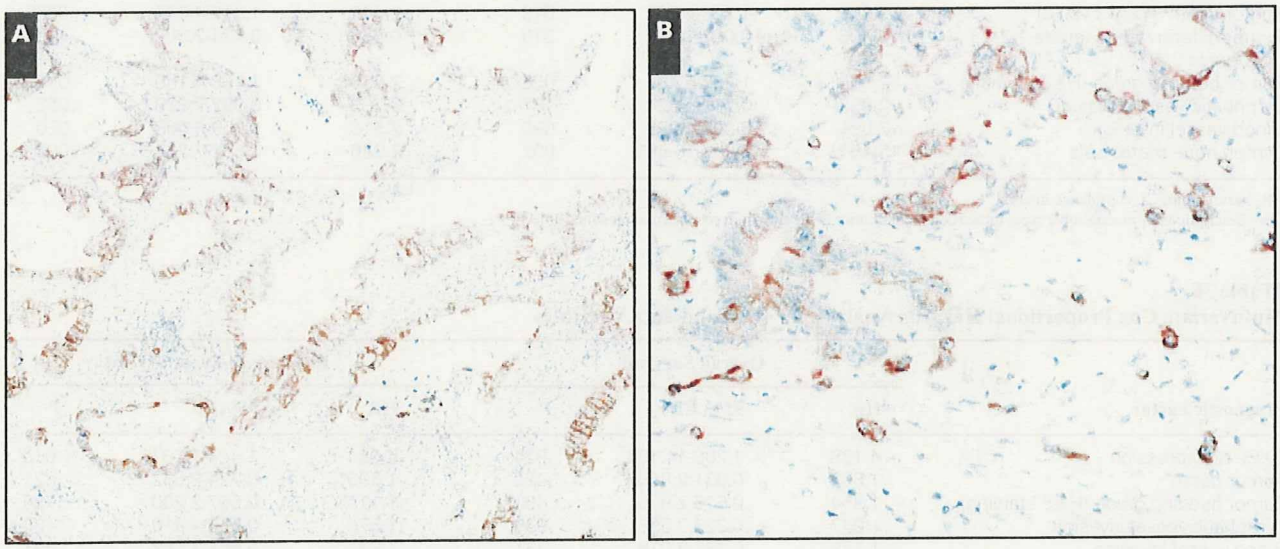

Image 1 Immunohistochemical studies of CXCL12 in colorectal carcinoma. **A**, CXCL12 expression was observed in the cell membrane and cytoplasm of colorectal tumor cells. In this case, almost all tumor cells expressed CXCL12 (×45). **B**, CXCL12 expression was intense in tumor budding foci at the invasive front (×230).

DOI: 10.1309/AJCPK35VZJEWCUTL

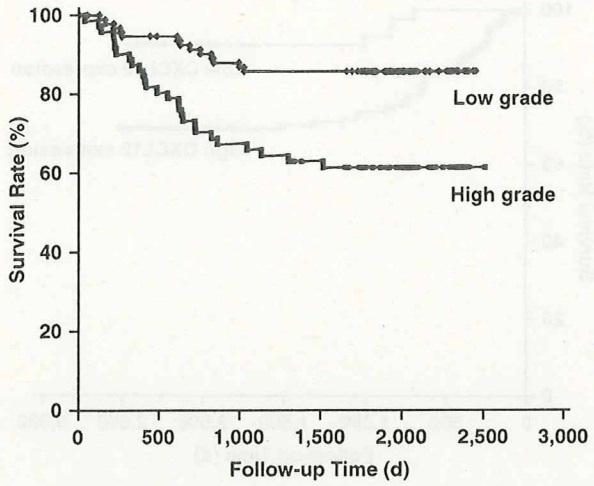

Figure 2 Kaplan-Meier survival curves of patients with colorectal carcinoma subdivided according to the grade of CXCL12+ tumor budding (P = .003; log-rank test).

staining (P < .001), lymph node metastasis (P = .003), and lung metastasis (P = .030) (Table 1). Univariate analysis using the Cox proportional hazards model revealed that the grade of CXCL12-immunopositive tumor budding was a significant prognostic factor (Table 2). Multivariate analysis using the Cox proportional hazards model revealed that only lymph node metastasis was an independent prognostic factor for overall survival and that CXCL12+ tumor budding grade was not an independent factor for overall or recurrence-free survival **Table 4**.

Combination of CXCL12 Expression and CXCL12+ Tumor Budding Grade

Patients with high CXCL12 expression and high-grade tumors had significantly shorter survival than patients with other combinations (P < .001 and P < .001, overall and recurrence-free survival rates, respectively; log-rank test) **Figure 3**. This combination was correlated with the depth of tumor invasion (P < .001), tumor budding grade by H&E

Table 2
Univariate Cox Proportional Hazards Analysis for the Candidate Variables*

	Overall Survival			Recurrence-Free Survival		
Prognostic Factor	**HR**	**95% CI**	***P***	**HR**	**95% CI**	***P***
CXCL12 expression	3.992	1.210-13.167	.023	3.991	1.420-11.219	.009
CXCL12+ tumor budding grade	3.036	1.420-6.493	.004	3.140	1.619-6.091	.001
CXCL12 expression and CXCL12+ tumor budding grade	3.540	1.655-7.574	.001	3.659	1.886-7.098	<.001
Age	1.013	0.538-1.906	.969	0.949	0.464-1.941	.885
Sex	1.139	0.609-2.133	.684	1.855	0.826-4.168	.134
Tumor location	1.118	0.573-2.430	.653	1.139	0.609-2.133	.684
Tumor size	1.119	0.546-2.293	.760	0.889	0.478-1.654	.711
Macroscopic type	0.977	0.278-3.429	.970	1.218	0.382-3.885	.740
Tumor depth (T2, T3 vs T4)	2.375	1.158-4.867	.018	2.442	1.312-4.544	.005
Tumor differentiation (grade 1/2 vs grade 3/4)	0.406	0.097-1.706	.219	0.556	0.134-2.307	.419
Tumor budding grade (H&E staining)	2.663	1.292-5.486	.008	2.230	1.198-4.150	.011
Lymphatic vessel invasion	2.032	0.709-5.824	.187	2.789	0.992-7.839	.052
Blood vessel invasion	2.081	0.893-4.853	.090	2.516	1.159-5.463	.020
Lymph node metastasis	5.454	1.902-15.639	.002	3.326	1.532-7.222	.002

HR, hazard ratio; CI, confidence interval.
* For descriptions of macroscopic type, tumor depth, and tumor differentiation, see the footnotes for Table 1.

Table 3
Multivariate Cox Proportional Hazards Analysis for the Candidate Variables

	Overall Survival			Recurrence-Free Survival		
Prognostic Factor	**HR**	**95% CI**	***P***	**HR**	**95% CI**	***P***
CXCL12 expression	4.138	1.209-14.168	.024	4.084	1.404-11.878	.010
Tumor depth*	1.332	0.621-2.856	.462	1.393	0.724-2.682	.321
Tumor budding grade (H&E staining)	1.354	0.616-2.975	.451	1.117	0.567-2.200	.750
Lymphatic vessel invasion	1.047	0.323-3.398	.939	1.576	0.516-4.810	.424
Blood vessel invasion	1.179	0.461-3.019	.731	1.535	0.657-3.582	.322
Lymph node metastasis	5.063	1.654-15.493	.005	2.781	1.200-6.444	.017

HR, hazard ratio; CI, confidence interval.
* For description, see the footnotes for Table 1.

DOI: 10.1309/AJCPK35VZJEWCUTL